

Simulated and reconstructed temperature in China since 1550AD

Jian Liu¹, Hans von Storch², Eduardo Zorita², Xing Chen^{3,1}, Sumin Wang¹

1. Nanjing Institute of Geography and Limnology, CAS, Nanjing 210008, P.R.China

2. Institute for Coastal Research, GKSS Research Center, 21502 Geesthacht, Germany

3. Department of Atmospheric Sciences, Nanjing University, Nanjing 210093, P.R.China

Abstract

In this paper, reconstructed decadal mean temperature anomaly series of 8 regions of China are compared to those generated in two multi-century simulations with a climate model, which was forced with time variable volcanic aerosols, solar output and atmospheric greenhouse gas concentrations. The two model simulations are rather similar but exhibit some differences. Both, the reconstructed and simulated developments of the temperature exhibit a “hockey-stick” pattern, with a marked increase of temperatures since the beginning of the 20th century. The variations of time scales of a few decades are, however, mostly dissimilar in the historical and proxy-based account and in the model data.

An attempt is made to assess whether the warming during the 20th century is within the range of “normal” variations related to solar and internal dynamical influences. It is found that the reconstructed data are well above the pre-industrial noise level of temperature fluctuations during most of the 20th century. Within the adopted framework, only the increased greenhouse gas concentrations can account for these significantly elevated temperatures

Key words: China, climate, temperature, climate model, climate change, detection

1 Introduction

Research of climate change since Little Ice Age (LIA, 1550-1850AD) has received extensive concern in China. Wide-spread and severe famine and serious social turmoil have taken place in China during the Little Ice Age (LIA) (Xu, 1998). Also the warm conditions after the LIA had great impact on human life and the national economy (Yang, et al. 2002). Because of this broad interest, the climate of China during the last 2000 years has been reconstructed by Chinese scientists, in particular temperature and precipitation since LIA with a variety of proxy data, such as historical documents, tree rings, ice cores, lake warves, archaeological materials, etc. (Wang et al., 1998; Wang and Gong, 2000; Liu and Cai, 2002; Liu and Ma, 1999, Liu and Shao, 2002, Zheng and Zheng, 1993; Yao et al. 1996).

Recently two long term climatic simulation experiments has been done by a consortium of scientists from Institute for Coastal Research, GKSS Research Centre and other institutions. The first run, named "Christoph Columbus" (CC) was run over 535 years beginning in 1450, and is described in some detail by Zorita et al. (2003). The second run, named "Erik den Røde" (EdR), was begun in 900 and ran over 1100 years. Both simulations were done with the same climate model ECHO-G with, however, different code versions adapted to different computer systems. Reconstructed time series of the radiative effect of the presence of volcanic aerosols, greenhouse gases in the atmosphere as well as variable solar output were used as forcing (see below). The modeling results reveal global and regional pattern of natural and anthropogenic climate change, which have some similarities with the observational record (Zinke et al., 2003, De Zolt et al., 2003). The purpose of the present study is to compare these simulated data with observational evidence for the territory of China, and to interpret the recent changes of Chinese temperatures in the context of the forced climate model.

In Section 2 we briefly introduce the reconstructed temperature data used in this comparison, and in Section 3 the simulations are sketched. In Section 4 the simulated and reconstructed historical temperature anomalies are compared. In Section 5, the warming in the last century is identified as being beyond the range of variations related to natural and internal causes, and in Section 6 the paper is concluded with a brief discussion.

2 Reconstructed temperature from China

Continental monsoon dynamics with complicated seasonal patterns is the major characteristic of China's present climate. The northerly monsoon prevails in winter, the southerly does in summer, the four seasons are very distinct, and the season of most of rainfall is summer. From every September to April of next year, the cold and dry winter monsoon blows from Siberia and Mongolia plateau to the mainland of China and weakens gradually from northwest to southwest, causing the cold and dry climatic state with a very great difference in temperature. The time of the wet summer monsoon control is shorter, from April to September. The warm and wet summer monsoon blows from the western Pacific and Indian Ocean, causing a state with the high temperature and much rain and little difference in temperature from north to south.

China can be divided into 10 districts (Wang et al., 1998a), which are relatively homogeneous in terms of temperature, precipitation and growing season. These are northeast of China, north of China, east of China, middle of China, south of China, southeast of China, southwest of China, northwest of China, Xinjiang region and Tibet region (Figure 1). With proxy data of historical documents, tree rings and ice cores available, reconstructions of temperature series have been made for all these regions, except regions of northeast of China and Xinjiang region. The reconstructions of 10-year mean temperature anomalies (relative to 1880-1979 averages) are based on proxies, such as temperature index, tree ring width and density, $\delta^{18}\text{O}$ of ice core, via statistical techniques which rely on establishing empirical relationships between modern observations and environments (Wang et al., 1998a). The proxy data and time series length of the reconstructed temperature anomalies can be found in Table 1. They are anomalies relative to 1880-1979.

The reconstructions have been compared with the empirical evidence available from the past century. Unfortunately, this evidence is very uncertain. One analysis of decadal mean temperatures has been prepared by Wang et al. (1998b), who used three kinds of data: from 1951-1996 CMA's monthly temperature series from 165 stations for whole China, from 1911-1950 CMA's temperature grade diagram series for 139 stations of China, and from 1880-1910 documentary data, ice core and tree-ring data. On the other hand, Jones et al. (1999) made an attempt to reconstruct Chinese temperatures from 1856 to 1998 AD. This reconstruction is rather uncertain, in particular before

1949 (Jones, pers. comm.). Both reconstructions deviate markedly from each other also in recent decades, as is demonstrated in Figure 2.

The fit of the historical data and the "observed" data is facilitated by using data from the Wang et al.-analysis (1998b). Unfortunately, we have no access to the original analyses by Wang et al. (1998b) except for region 3. Also, robust measures of skill of this reconstruction are not available either, and it seems plausible that the very good fit shown in Figure 2 is the result of overfitting. Unfortunately we have no means to assess which of the two reconstructions (Wang and Jones) is more skilful, nor to do our own analysis with the raw data; therefore we have to rely on the published results, even if we have some doubts about the methodology.

We therefore adopt the pragmatic, and to some degree admittedly questionable standpoint that Wang's reconstruction is essentially valid on time scales of several decades of years, e.g., 5-decade running means. The root mean square difference between the 5-decade running means given by the historical reconstruction (based upon historical evidence and geoscientific proxies, fitted to the unavailable Wang et al. (1998b) data set) and Jones et al. (1999) varies between 0.13 K and 0.36 K in the eight regions, and averaged to 0.24 K for all regions. We consider this number a crude but educated estimate of the inherent uncertainty of the historical temperature variations in China on the time scale of 50 years.

The time-averaged time series are shown in Figure 3. They all share a marked warming since about 1900 by 0.5 K and more. In 7 out of the 8 regions, the last decades are associated with a cooling, only in region 4 the warming is continuing. In the time before 1900 the temperatures vary very differently in the 8 regions. In particular region 7 and 8, for which the estimates are based upon not on historical data but on geoscientific proxy data (Table 1), exhibit rather strong negative temperature swings, with additional temperature differences to the warmer regions by 0.5 K. It is not entirely plausible that the temperature variations are so unconnected even on time scales of 50 and more years. In fact, the variations simulated in the climate model are much more uniform, but it is unclear if this is a realistic property or not.

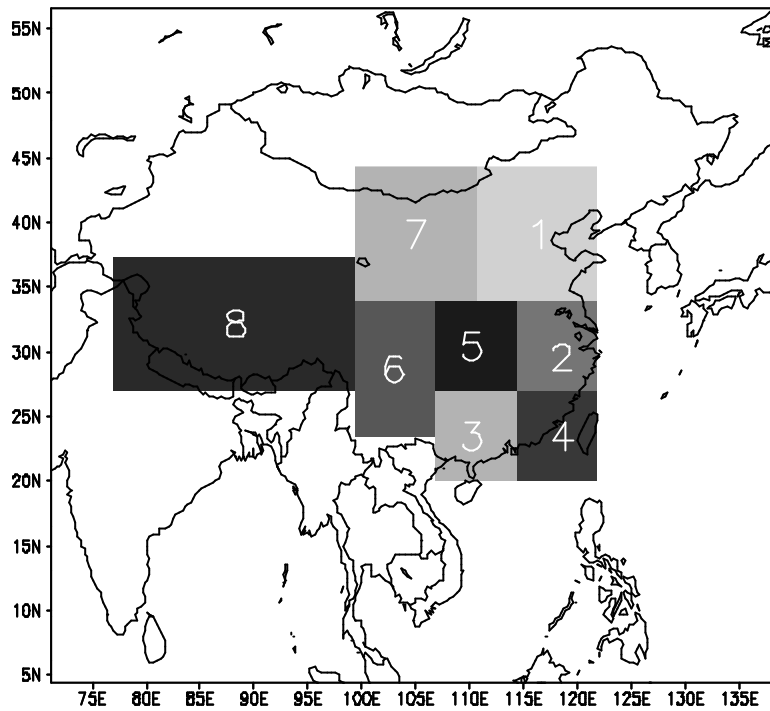


Figure 1. Regions of China with reconstructed temperature series

Table 1 : Proxy data and reconstructed series length of 8 regions . (Wang et al., 1998a)

No.	Region	Proxy data	Length
1	North of China	Historical materials	1380-1990
2	East of China	Historical materials	1380-1990
3	South of China	Historical materials	1500-1990
4	Southeast of China	Historical materials	1500-1990
5	Middle of China	Historical materials	1470-1990
6	Southwest of china	Historical materials	1500-1990
7	Northwest of China	Ice cores	1000-1990
8	Tibet Region	Tree rings	1000-1990

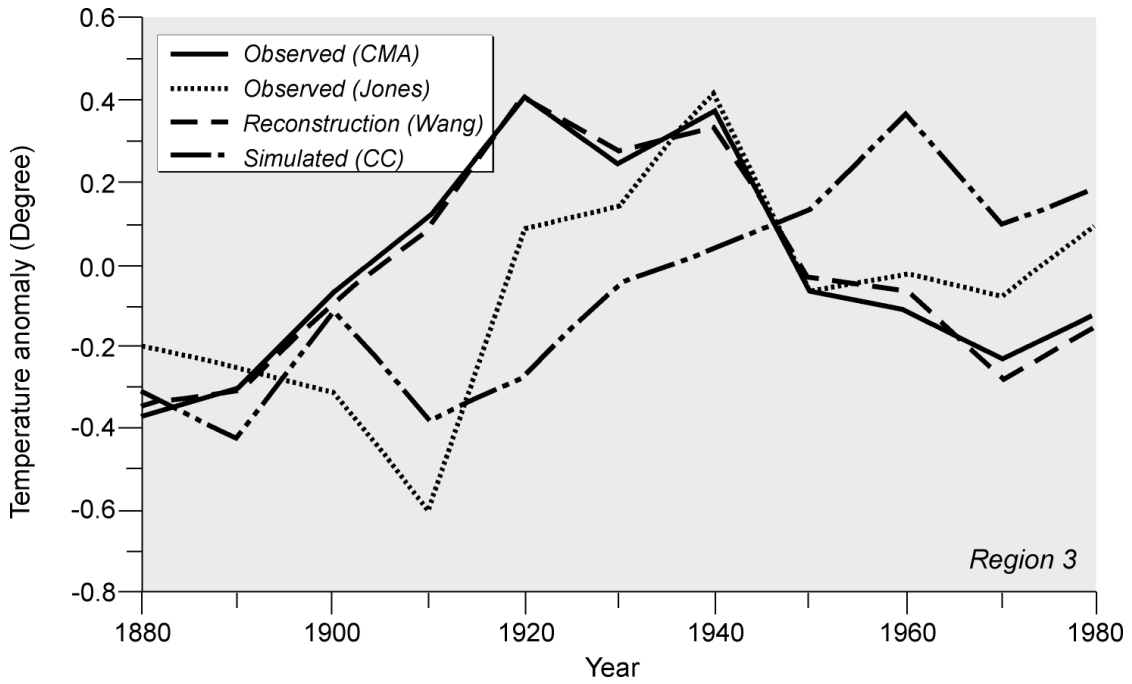


Figure 2: Conflicting assessment of decadal mean temperature fluctuations in region 3 of China – according to the Wang et al. (1998b) analysis of mainly instrumental data (CMA data), Jones et al. (1999), the historical reconstruction by Wang et al. (1998a), and the CC simulation with ECHO-G. The decades are labeled by the first year of a decade, e.g., 1920 stands for the years 1920-29.

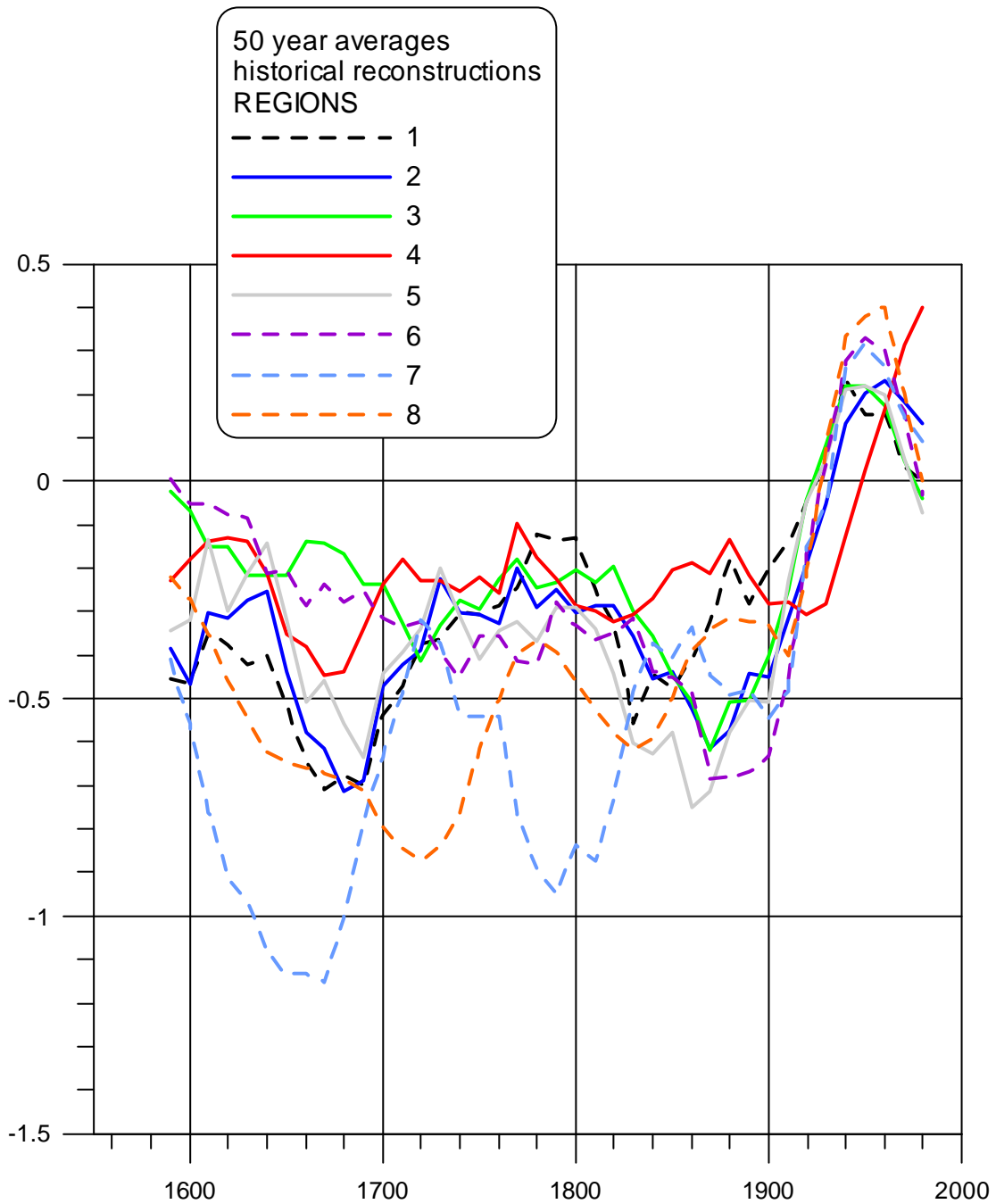


Figure 3: Time series of reconstructed, temporarily smoothed mean temperatures for the 8 regions shown in Figure 1. A running mean filter, averaging 5 consecutive decadal means is applied so that efficiently 50 years means are shown.

3 ECHO-G simulations, 1550-2000

Two multi-century integrations has been performed with the state-of-the-art climate model ECHO-G, which is a combination from the ocean model HOPE-G in T42 resolution and the atmospheric model ECHAM4 in T30 resolution both developed at the MPI in Hamburg (Legutke and Voss, 1999). Two runs, named “Christoph Columbus” (CC) and “Erik den Røde” (EdR) were executed, one over 535 years and another over 1100 years. The runs were exposed to time-variable external forcing related to solar and volcanic activity and changing atmospheric concentrations of greenhouse gases. The CO₂ and methane atmospheric concentrations were derived from air trapped in Antarctic ice cores (Blunier et al., 1995; Etheridge et al., 1996). The variations of solar output and the influence of volcanic aerosols on the radiative forcing were derived from the number of sun spots after 1600 AD and concentrations of cosmogenic isotopes in the atmosphere before 1600 AD (Crowley, 2000). The forcing due to volcanic aerosols was estimated from concentrations of sulphuric compounds in different ice cores, located mainly over Greenland. These forcing factors were then translated to effective variations of the solar constant in the General Circulation Model (GCM) taking into account the corresponding geometric factors and the mean earth albedo. Changing loading of industrial aerosols has not been incorporated in the simulation.

In the following we consider only the time simulated in both runs, namely 1550 to today. Figure 4 shows for this time the history of the effective solar activity, greenhouse gas and volcanic-aerosol concentrations used to force the model. Also the global mean near-surface temperature is shown.

The CC model integration was started in year 1465 AD with the forcing conditions of 1990 and slowly driven in a 30 year transition period to the corresponding solar, volcanic-aerosol and greenhouse gas concentrations estimated for 1500 AD. The model attained an equilibrated state in about the model year 1550. The EdR simulation was started in the year 900, and the model attained its new equilibrium within the first 100 years of the ntegration.

The CC simulation is described in some detail by Zorita et al. (2003), its consistency with observational evidence during the Late Maunder Minimum is described by Zinke et al. (2004), and the relationship between forcing on the one side, and the NAO and European temperature on the other side by de Zolt et al. (2003). Aspects of the EdR run are presented in González-Ruoco et al.

(2004). The material presented in the following is demonstrating that the temperatures in China simulated in the two runs are rather similar, even though during the period up to about 1700 EdR seems to be in some regions systematically cooler than CC.

The simulated data are available on a grid with about 300 km mesh size. The data are spatially averaged to obtain spatial mean values for the eight larger boxes shown in Figure 1.

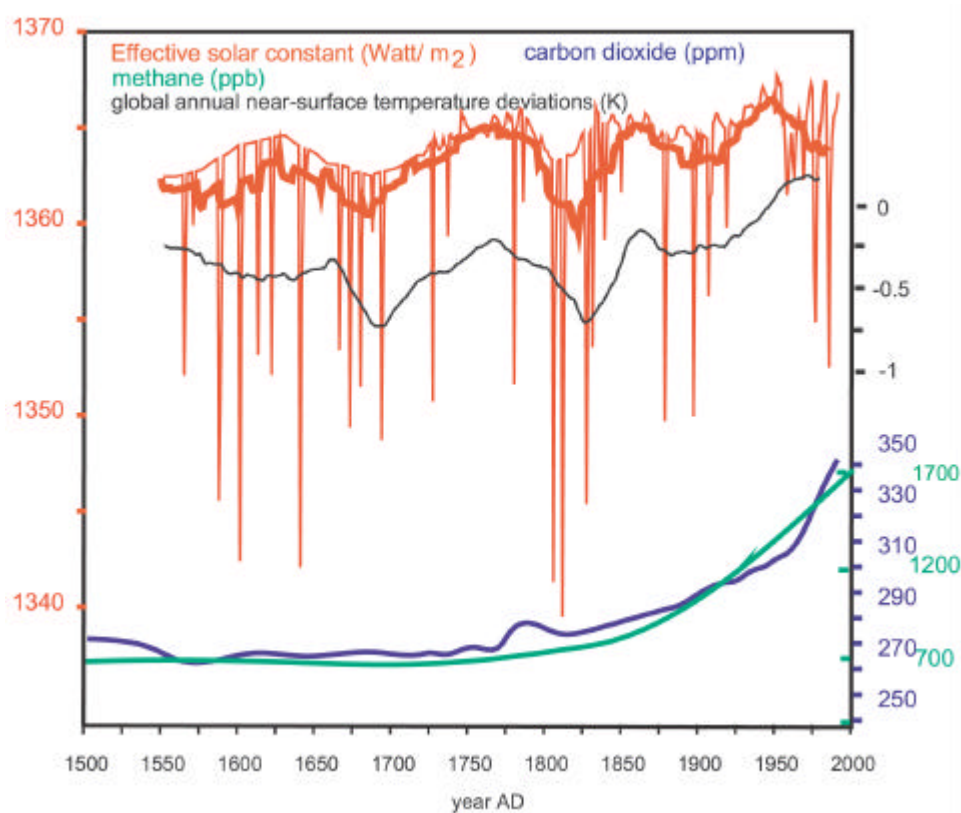


Figure 4: Time series of simulated global mean temperature (black) in the CC simulation, of atmospheric methane and carbon dioxide concentration and effective solar constant (red), mimicking the presence of volcanic aerosols and a variable solar output used in both CC and EdR.

4 Comparisons between modelling results and reconstructions

All data are anomalies relative to the 10-decades (1880-1889, 1890-1899, ... 1970-1979) mean. The decades are labeled by the first year, .e., 1980 represents the years 1980-89.

We first examine the past century, because during that time the temperature estimates are based mostly on direct observations. During that time we consider decadal (10 year mean) data. In a second step, we consider the longer perspective, when only the reconstruction by Wang et al. (1998a) is available.

Previous analyses (de Zolt et al., 2003) have shown that the solar and volcanic forcing is not strong enough to imprint a strong signal on time scales of years to a few decades. Therefore, we limit our comparison to multi-decadal time scales – specifically to 5-decade running mean values (i.e., averages of 5 consecutive 10 year means). It is hoped that this smoothing will overcome also in part the inherent uncertainty of this reconstruction.

4.1 Comparison with instrumental data, 1880/1920-1979

Here we compare decadal mean temperatures for the eight boxes as simulated in the model and as estimated from historical and geoscientific evidence (Wang et al., 1998a).

The bias between the reconstructed and simulated box-mean temperatures varies between 0.07 K and -0.15 K, which is, however, considerably less than the systematic difference between Wang's estimate and Jones' estimate of 0.16 K and -0.34 K. For the root mean square error a similar result is found. The rmse between Wang's estimate and the simulated data is on average 0.30 K, with a maximum value of 0.34 K, while the two estimates differ by 0.45 K on average, and a maximum value of 0.58 K. Thus the difference between model and reconstruction seems insignificant when compared with the inherent uncertainty of the historical reconstructions.

Since 1920 the Jones' instrumental data have relatively few gaps. Therefore we compare for this time the variances as given by Wang's reconstruction,

Jones reconstruction and the model output (Table 2). The simulated temperature variations are usually similar to Jones' data, with the largest difference in region 8, the Tibetan region, where the model simulates a variance up to fourtimes the variance deduced from instrumental observations. In case of the Wang's reconstructed data, the variance is in 6 out of 8 cases larger than the instrumental variance, which is insofar surprising as the reconstructed data are derived from a regression, which underestimates variance. The largest difference is again found for the Tibetan region, but this time the factor amounts to fifteen. Again, the simulated data are consistent with the observational evidence, if we use the discrepancy between the two reconstructions as a measure of uncertainty.

We will later see that this consistency of the model data is mainly due to the strong warming trend in the past century, which is well captured by all three data sets, Wang's reconstruction and the two model simulations.

Region	1	2	3	4	5	6	7	8
reconstructed	0.15	0.05	0.07	0.08	0.10	0.17	0.20	0.30
CC simulated	0.15	0.05	0.04	0.05	0.05	0.08	0.11	0.08
EdR simulated	0.14	0.06	0.02	0.02	0.03	0.04	0.05	0.03
Jones' estimation	0.20	0.07	0.04	0.06	0.06	0.05	0.08	0.02

Table 2: Variances for the 8 regions since 1920 (10 year mean values)

4.2 Comparison of reconstructed and simulated data, 1550-2000

The 50 year running mean temperatures for the eight regions (Figure 1) as reconstructed by Wang et al. (1998a) and as simulated by the two ECHO-G runs CC and EdR are shown in Figure 5. The inherent uncertainty of the reconstructions, as estimated from the root mean square difference between Wang et al.'s (1998a) analysis of 20th century temperature variations and Jones et al.'s (1999) analysis is shown as well. Note that the rmse is the expected mean error, i.e., in about half of the time, the error would be larger than the rmse, and in the other half of time larger. Thus it is a much less stringent error margin than a 2-s confidence band.

In all cases, the warming trend since about 1900 is shared by the

reconstructed temperatures and the simulated changes. In all 8 regions, both simulations warm with a rate of about 0.4-1.1 K/(100 a), whereas in Wang et al.'s reconstructions the warming is considerably weaker, -0.05 – 0.4 K/(100 a), which may be due to a significant cooling caused by the emissions of industrial aerosols, which is not accounted for in the GCM simulations. An exception is region 4, in SE China, where the reconstructions reveal a heating of 1.3 K/(100 a), and the GCM runs 0.5 and 0.8 K/(100 a).

In the pre-industrial time (1590-1910), the GCM simulates temperatures lower than Wang's estimates. In particular in the regions 1, 2, 5 and 6, the differences are larger than the rmse. Only in the regions 4 (SE China) and 8 (Tibet) the simulated temperatures vary within plus/minus one rmse. In case of Tibet the coincidence between the GCM and the proxy data is excellent. Also, the development in the Northwest, in region 7, is similar, even if the low-frequency variations are different. In the GCM world, temperatures vary around a level of -0.5 K and less, while the reconstructed temperatures vary around a level of -0.3 K or decline from a value close in 1550 to zero to a minimum in the late 19th century (regions 3 and 6 in Central and Southern China).

In general, the decadal variations are dissimilar in the reconstructed data and in the simulated data, even though the data are already heavily smoothed with a 5 decade running mean filter. The correlations between the reconstructed data and the CC-simulation for the entire period, 1590-1980, is positive (0.47 – 0.84), but these high values are essentially reflecting the presence of the hockey-stick pattern. If the two periods, pre-industrial 1590-1910 and industrial 1920-1980 are considered separately, the correlations become much smaller, namely -0.32 (region 6) to 0.72 (region 8) for the pre-industrial times, and -0.17 (region 1) to 0.32 (region 7) in modern times. (Because of the heavy serial correlation in the data, the determination of significance levels is not meaningful.)

Interestingly, the simulated curves are among themselves rather similar, quite differently from the large region-to-region variations displayed in Figure 3 for Wang's reconstruction.

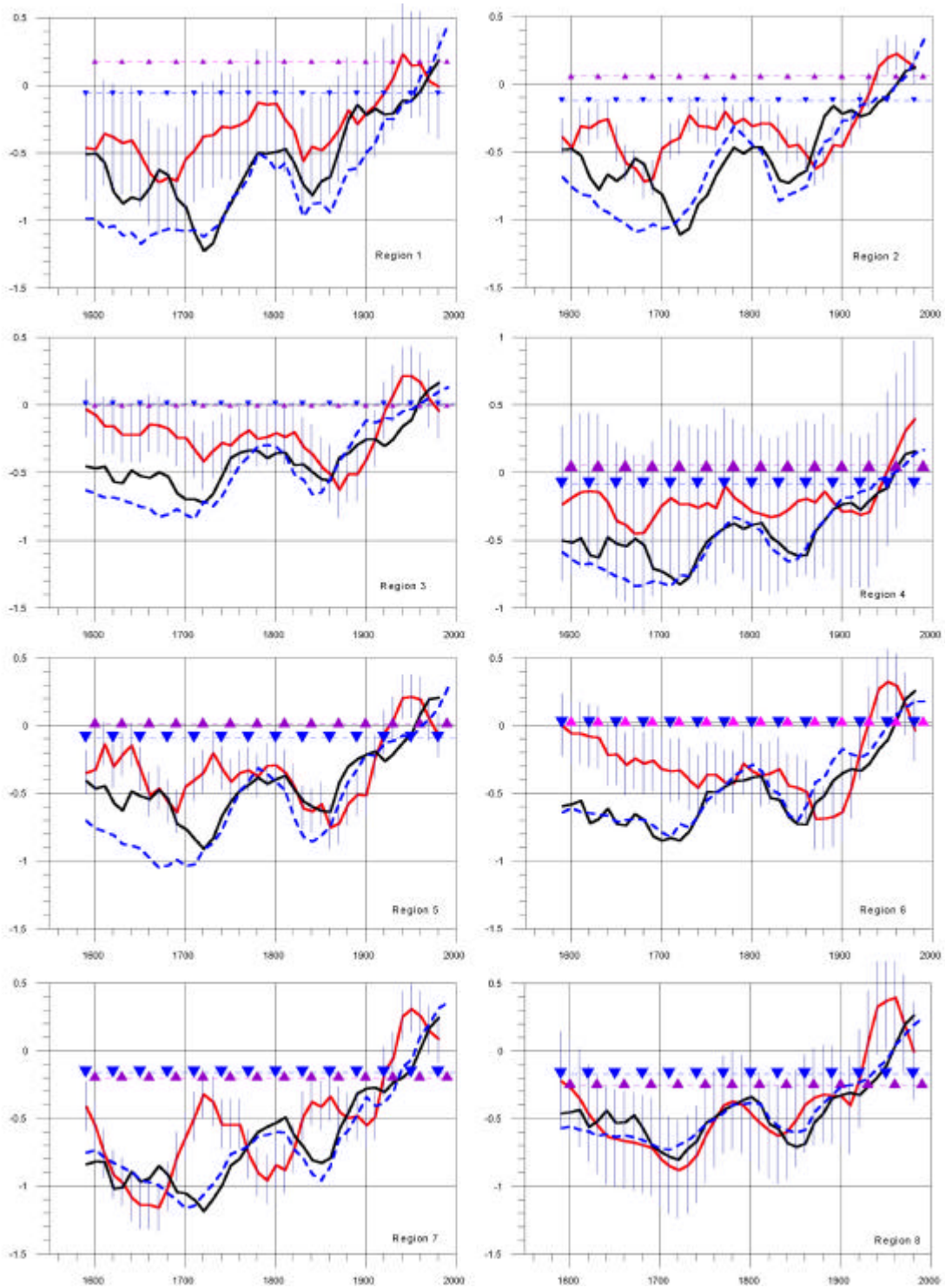


Figure 5 Comparisons of reconstructed (red) and simulated (black: CC; blue-dashed: EdR) 5-decade running mean temperature anomaly series for 8 regions of China as given in Figure 1. The uncertainty (vertical hatching) of the reconstructed temperature variations (Wang et al., 1998) is estimated by the rmse between the reconstructed values by Wang et al (1998) and those obtained by Jones et al. (1999) since 1880.

The horizontal lines with triangles indicate thresholds estimated to represent the expected range of natural variations, as estimated from Wang et al.'s reconstructions (downward triangles) and as estimated for the CC simulation (upward triangles).

The 5 decade running means are labeled by the last decade, .e., 1980 refers to 1940-1989.

4.3 EOF analysis

An EOF analysis is used to determine the joint spatial variability of the 5-decade running mean temperature for the entire time period 1590-1980. The EOFs are normalized so that the time series have a standard deviation of one, so that the magnitude of the signals is given by the patterns.

Not unexpectedly is one EOF enough to explain the bulk of the variations, namely 86% in case of the historical reconstruction, and 99% for the two GCM data sets (Table 3). In case of the historical data, two more EOFs carry a noteworthy amount of variance, namely 5% each. As already mentioned is the synchronicity in the reconstructed data weaker than in the GCM data (cf. Figure 5). It is unclear if this greater spatial variability (or, in other words, the larger degrees of freedom) is reflecting real temperature variations, or if it is due to insufficiencies of the reconstruction process.

The EOF is describing a synchronous warming, or cooling, in all eight regions. The loadings in the GCM EOF are higher than in the reconstructed data EOF. This is to some extent due to the fact that less variance is described, but it is also reflecting the fact that large swings in the simulated temperature, as for instance in the early 18th century are absent in the reconstructed data. Again, the similarity is best in case of Tibet (region 8).

The time series associated with the first EOF modes of simulated and reconstructed data is shown in Figure 6. The correlation coefficient of these two series is 0.80. The overall similarity is remarkably large, in particular with

respect to the century-time scale changes, but time scales shorter than a century, the time series differ substantially. Again the hockey-stick pattern emerges clearly. Note that the similarity in the range of variation is caused by the normalization of the EOFs.

Region	1	2	3	4	5	6	7	8	Described variance (%)
reconstructed	0.36	0.38	0.25	0.24	0.38	0.31	0.63	0.53	0.86
Christoph Columbus	0.65	0.59	0.44	0.48	0.50	0.56	0.74	0.50	0.99
Erik the Red	0.82	0.70	0.54	0.55	0.67	0.53	0.75	0.50	0.99

Table 3: First EOF of reconstructed and simulated temperature in the eight regions. Prior to the EOF analysis, the data are smoothed with a running 5-decade filter. The EOFs are normalized so that the time coefficients (Figure 6) have a standard deviation of 1.

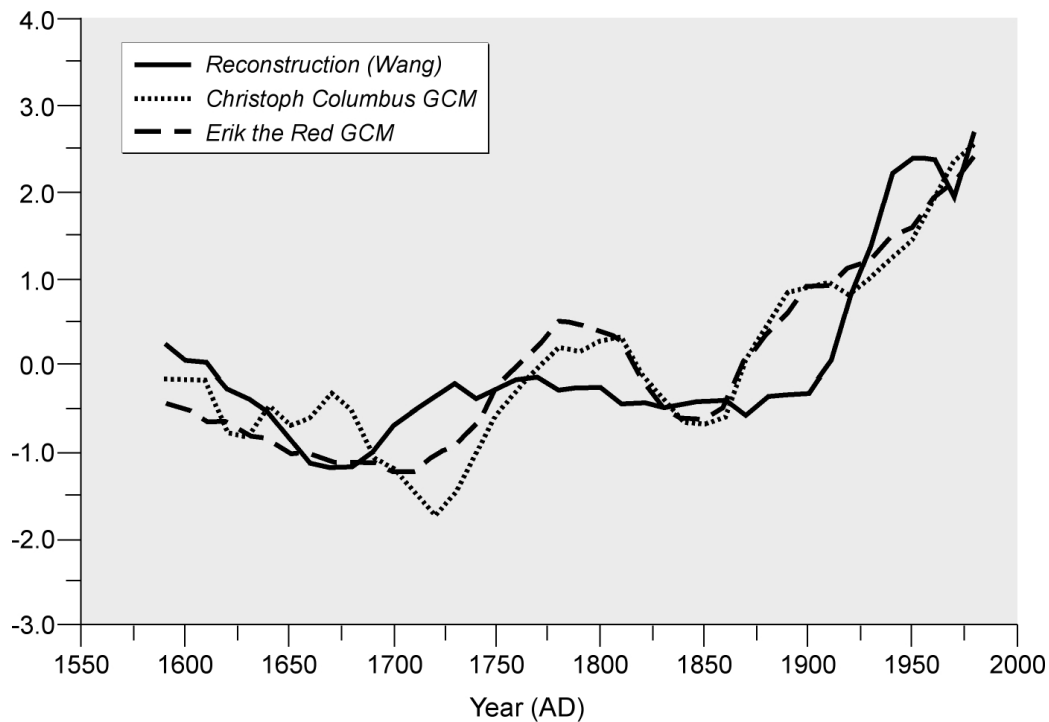


Figure 6: Time series of the first EOF coefficients of 5-decade running mean simulated and reconstructed temperature. Note that the EOFs are normalized to standard deviation 1, so that the patterns (in Table 4) carry the different magnitudes of variations. The 5-decade running man values are labeled by he last considered decade, so that 1970 refers 1930-1979.

5 Assessment of the warming during the last century

The similarity of the century scale variations in the reconstructions and in the GCM output is remarkable. The main feature of the similarity is the relatively stationary conditions until about 1900, on top of which significant decade-to-decade variations are taking place.

In the GCM, these variations are related to changing forcing conditions, as displayed in Figure 4. The variations in volcanic activity contribute mostly to variations, which extend only over a few years. The solar activity contributes to variations on all time scales, but the dominant signal is exerted by the increasing greenhouse gas concentrations in the 20th century.

The question is if the reconstructed record may be interpreted similarly. This is the “detection and attribution” problem (Hasselmann, 1979; Hegerl et al., 1997; Zwiers, 1999). That is, one has first to demonstrate that the recent warming is beyond the variations one would expect from “natural variations”, i.e. variations prior to 1910 due to natural and internal causes. Next, one has to demonstrate that the recent decades warming trend is consistent with the simulated response to the given forcing, i.e., to the forcing spectrum given in Figure 4.

5.1 Detection

To do so, we first determine the variability of the smoothed temperature time series displayed in Figure 5 during pre-industrial times, and compare these with the changes which have taken place in the 20th century. In Table 4, the mean value of Wang’s reconstruction for 1590-1910 is listed together with the standard deviations for that time in Wang’s reconstruction as well as in the two simulations. We consider this period of 1590-1910 as “pre-industrial time”, which is not significantly affected by anthropogenic factors.

The level of variability during pre-industrial time is mostly consistent in the reconstructions and in the GCM simulations, even though there are sometimes larger differences. We consider a temperature above the range of “normal” variations, when it is larger than the mean plus two standard deviations. This “pre-industrial” noise level, as given by the mean value

derived from the reconstructions plus 2 standard deviations, taken from either the reconstructions or from the CC simulations, is displayed in Figure 5 by horizontal lines marked with triangles.

parameter	data	1	2	3	4	5	6	7	8
time mean	Wang et al. reconstruction	-0.38	-0.40	-0.27	-0.24	-0.41	-0.34	-0.68	-0.53
standard deviation	Wang et al. reconstruction	0.16	0.14	0.14	0.08	0.16	0.18	0.26	0.18
standard deviation	CC GCM	0.27	0.23	0.13	0.15	0.17	0.16	0.24	0.14
standard deviation	EdR GCM	0.22	0.26	0.21	0.20	0.26	0.18	0.21	0.13

Table 4: Characteristics of 5-decade running mean temperature during the pre-industrial time 1590-1910 in the eight Chinese regions. Wang et al.'s reconstruction (mean and standard deviation; top two rows) and GCM simulations CC and EdR (standard deviations; bottom two rows)

Region	times with significantly elevated temperatures
1	1920-1980
2	1930-1980
3	1930-1970
4	1950-1980
5	1930-1980
6	1940-1960
7	1920-1980
8	1920-1980

Table 5: Times during which the 5-decade running mean temperature reconstructed by Wang et al. (1998) is above the "pre-industrial noise level", given by mean plus 2 standard deviation for the time 1590-1910.

The times when the reconstructed temperature is beyond the 1590-1910 average plus 2 standard deviations are listed in Table 5, with the parameters given in Table 4. On average, about 98% of all pre-industrial temperatures should be below this level. In fact, this estimate of the pre-industrial noise level is conservative, as all temperatures were beyond this level (Figure 5). This is due to the skewness of the temperature distribution.

In all 8 regions, most of the 20th century temperatures were above the pre-industrial noise level, defined by either the CC model data or Wang et al.'s reconstructions (Figure 5). If the standard deviations derived from Wang's reconstruction are replaced by the larger standard deviations derived from the pre-industrial periods in the GCM simulations, similar noise levels are obtained (Figure 5) – with the same overall conclusions, namely that during most of the 20th century the reconstructed temperatures are significantly elevated compared to the pre-industrial period 1590-1910.

Thus, we conclude that the recent warming in China, as it is documented in Wang et al.'s (1998a) reconstruction, is beyond the range of natural variations, and that an explanation of the phenomenon requires the consideration of other factors, in particular increased levels of atmospheric greenhouse gas concentrations.

5.2 Attribution

In order to assess the likelihood that greenhouse gas forcing would be responsible for the recent warming; a simple statistical model for the temperature evolution is fitted to the output of the GCM simulation for each of the eight boxes:

$$(*) \quad T_{t+1} = aT_t + \beta S_t + \gamma \log(C_t) + n_t$$

Here, T_t is the smoothed temperature deviation from the pre-industrial mean (1590-1910; given in Table 4); S_t is the time-variable solar forcing deviation from the pre-industrial mean 1590-1910, and C_t the time variable deviation in greenhouse gas concentrations, n_t stands for the remainder which is considered in this context as noise. The coefficients a , β and γ are determined so that the model variations are best described:

Region	a	b	g
1	0.604	0.118	1.697
2	0.643	0.087	1.562
3	0.867	0.009	1.365
4	0.740	0.039	1.272
5	0.709	0.064	1.443
6	0.962	-0.008	1.351
7	0.714	0.040	1.306
8	0.836	0.043	1.456

A direct comparison of the three parameters is not possible since the variance of the temperature itself and of the two forcing factors is different. However, the memory term aT_t is the most important – the very magnitude of a is due to the heavy smoothing by the 5-decade running mean filter. The influence of the solar forcing is varies substantially between the 8 regions, and in one case the fit results even in a physically implausible negative value – indicating that the fit may suffer somewhat from estimation problems. The parameter g -coefficient is similar in the eight boxes.

The model is linear, so that sum of the response T_t^s to solar and volcanic forcing alone and of the response T_t^c to greenhouse gas forcing alone equals the response to both forcings, if the noise is disregarded and both are integrated with the same initial value T_{1590} . Therefore, equation (*) allows an estimate of the relative importance of the two forcing factors. In the following table, we list the reconstructed change of temperature according to Wang et al. (1998a), the change estimated through (*) to solar and volcanic forcing alone, to greenhouse gas forcing alone, and to both of them. These are all deviations from the pre-industrial values (1590-1910)

Region	1	2	3	4	5	6	7	8
Wang et al. (1998a)	0.47	0.49	0.36	0.28	0.50	0.47	0.81	0.70
(*) with $S_t=0$	0.48	0.47	0.69	0.47	0.50	0.72	0.69	0.45
(*) with $\log C_t=0$	0.59	0.45	0.04	0.23	0.38	-0.18	0.31	0.23
(*) with both forcings	1.08	0.93	0.73	0.70	0.88	0.58	1.00	0.68
Ratio Wang/(*)	0.44	0.53	0.49	0.40	0.57	0.81	0.81	1.02

When comparing the historical warming with the estimated warming (2nd and 5th row) we find that (*) gives higher values. The ratio of the two numbers (last row) varies between 0.40 in the eastern part of China and 1.02 in the western part. We suggest that this overestimation by model (*) reflects the increasing cooling effect of regional emissions of industrial aerosols, which have strongest in the densely populated east and south of China, while the western part of China experiences less increasing emissions.

Apart of region 1, the estimated warming due to solar and volcanic effects (4 row) is smaller than the estimated anthropogenic greenhouse effect (3rd row). Only the anthropogenic greenhouse effect is strong enough to explain the observed warming, in spite of the fact that the latter is considerably reduced by the unaccounted effect of the increasing industrial aerosol impacts.

We conclude that the total estimated response is consistent with the empirical evidence in terms of sign and, to a lesser extent, with magnitude. The major part of the 20th century warming can be explained only with the help of the anthropogenic greenhouse gas effect, whereas the solar effect can account only for a smaller proportion. Differently from the development in the GCM simulations, which is a steady upward trend throughout the 20th century, there is in the reconstructions a decline in the 2nd half of the 20th century. We suggest that this is reflecting the steady increase of industrial aerosol emissions (Krüger, pers. communication) in China.

6 Conclusions

We have analyzed Wang et al.'s (1998a) reconstruction of regional temperatures in China since the 16th century with respect to traces of the impact of changing forcing conditions. We found that the reconstructed temperatures are reasonably well simulated by a climate model subject to time-variable solar, volcanic and greenhouse gas forcing. The similarity is good on time scales of a century, while the model generates variability on shorter time scales without a counterpart in the reconstructions.

The development of regional temperature in the recent decades of the industrial period is towards significantly elevated levels – where the significance is assessed by comparing against a pre-industrial “normal” and “noise level”. Thus, the presence of non-normal external factors must be assumed. Using the GCM simulations to assess the relative importance of the solar and volcanic as well as greenhouse gas forcing, we find that only the greenhouse gas forcing can account for the recent warming.

There are a number of potential sources for errors. The most severe is the reliability of the historical reconstructions of regional temperature in China. These temperature are rather uncertain not only because of the usual uncertainties in data derived from, for instance, tree ring width, but also since the data base of instrumental data to build the empirical transfer functions is not good. Other caveats refer to the model simulations. For instance, the inclusion of the volcanic effects is relatively rough. Also, the effect of industrial aerosols of cooling the regional atmosphere is not represented in the model simulations. Finally, the utilized forcing factors suffer from uncertainties.

7 Acknowledgements

Financial support was provided by the Natural Sciences Foundation of China (40272123), the Chinese Academy of Sciences (KZCX3-SW-321) and by the GKSS Research Center in Geesthacht, Germany. Valuable help and advice was given by Fidel González-Ruoco and Olaf Krüger. Beate Gardeike helped professionally with the diagrams.

8 References

Blunier, T., J.A. Chappellaz, J. Schwander, B. Stauffer, and D. Raynaud. 1995. Variations in atmospheric methane concentration during the Holocene epoch. *Nature* 374:46-49

Crowley, T.J., 2000: Causes of climate change over the past 1000 years. *Science* 289, 270-277

De Zolt, S., P. Lionello, J. Luterbacher and E. Zorita, 2003: The variability of the winter European climate and the NAO index during the last 500 years. (in preparation)

Etheridge D., L.P. Steele, R.L. Langenfelds, R.J. Francey, J.M. Barnola, V.I., 1996: Morgan Natural and anthropogenic changes in atmospheric CO₂ over the last 1000 years from air in Antarctic ice and firn. *JGR*. 101, 4115-4128

González-Ruoco, J.F., H. von Storch and E. Zorita, 2004: Deep soil temperature as proxy for surface air-temperature in a coupled model simulation of the last thousand years. *Geophys. Res. Letters*, in press

Hasselmann, K., 1979: On the signal-to-noise problem in atmospheric response studies. *Meteorology over the tropical oceans* (B.D. Shaw ed.), pp 251-259, Royal Met. Soc., Bracknell, Berkshire, England.

Hegerl, G.C., K.H. Hasselmann, U. Cubasch, J.F.B. Mitchell, E. Roeckner, R. Voss and J. Waszkewitz, 1997: Multi-fingerprint detection and attribution analysis of greenhouse gas, greenhouse gas-plus-aerosol and solar forced climate change. *Clim. Dyn.* 13, 613-634

Jones PD, M. New, D.E. Parker et al. 1999: Surface air temperature and its changes over the past 150 years. *Reviews of Geophysics*, 37: 173-199

Legutke, S., and R. Voss, 1999: The Hamburg atmosphere-ocean coupled circulation model ECHO-G. Technical Report No. 18, DKRZ, Hamburg

Liu H-B. and Shao X-M, 2002: Reconstruction of the dry index series of early summer during the last 500 years within the Pass area of Shaanxi of China and adjacent area. *Quaternary Sciences* 22(3), 220-229 (in Chinese)

Liu Y, and Cai Q-F, 2002: Tree ring precipitation records and changing of eastern Asian summer monsoon — Taking Baotou area of the Inner Mongol as an example. *Front of Earth Sciences* 8(1): 91-97 (in Chinese)

Liu Y, and Ma L-M, 1999: Reconstruction of seasonal precipitation from

tree ring width of Huhehaote during the last 376 years. Chinese Science Bulletin 44(18): 1986-1992 (in Chinese)

Wang, Sh-W, Ye J-L, and Gong D-Y, 1998a: Climate of Little Ice Age in China. Quaternary Sciences (1): 54-64 (in Chinese)

Wang Sh-W, Ye J-L, Gong D-Y, Zhu J-H, and Yao T.D, 1998b: Construction of mean annual temperature series for the last one hundred years in China. Quarterly Journal of Applied Meteorology, 9(4): 392-401 (in Chinese)

Wang Sh-W, Gong D-Y, 2000: Temperatures of China in several typical periods of Holocene. Progress in Natural Science, 10(4) 325-332 (in Chinese)

Xu J-H, 1998: Sun, climate, famine and national migration. Science in China (series D) 41(5) 449-472

Yang B et al. 2002: Research progress on climate change during the last 2000 years. Progress in Earth Science 17(1): 110-117 (in Chinese)

Yao T-D, D-H. Qin, L-D. Tian, et al. 1996: Variations in temperature and precipitation in the past 2000a on the Tibetan Plateau: Guliya ice core record. Science in China (series D), 39(4): 425-433

Zheng, J-Y, and Zheng S-Zh, 1993: States of cold, warm, drought and waterlogging of Shandong province during historical period. Journal of Geography 48(4) 348-357 (in Chinese)

Zinke, J., H. von Storch, B. Müller, E. Zorita, B. Rein, H. B. Mieding, H. Miller, A. Lücke, G.H. Schleser, M.J. Schwab, J.F.W. Negendank, U. Kienel, J.F. González-Ruoco, C. Dullo and A. Eisenhauser, 2004: [Evidence for the climate during the Late Maunder Minimum from proxy data available within KIHZ](#). In H. Fischer, T. Kumke, G. Lohmann, G. Flöser, H. Miller, H von Storch und J. F. W. Negendank (Eds.): *The KIHZ project: towards a synthesis of Holocene proxy data and climate models*, Springer Verlag, Berlin - Heidelberg - New York, (in press)

Zorita, E., H. von Storch, F. González-Rouco, U. Cubasch, J. Luterbacher, S. Legutke, I. Fischer-Bruns and U. Schlese, 2003: [Simulation of the climate of the last five centuries](#), GKSS Report 2003/12, 43 pp.

Zwiers, F., 1999: The detection of climate change. In: H. von Storch and G. Flöser (Eds.): *Anthropogenic Climate Change*. Springer Verlag, 163-209, ISBN 3-540-65033-4